

Supplementary Information

Fluorescence immunoassay for targeted determination of trace *Listeria monocytogenes* based on immunomagnetic separation and CdZnTe quantum dots indication

Shan Liang, Li Ji, Yingying Zhong, Tiantian Wang, Huiyi Yang, Qing-Lan Li*,
Xiangguang Li* and Suqing Zhao*

*Department of Pharmaceutical Engineering, School of Biomedical and Pharmaceutical
Sciences, Guangdong University of Technology, Guangzhou 510006, People's
Republic of China*

*Corresponding Author

Dr. Qing-Lan Li

E-mail addresses: qli19@gdut.edu.cn

Prof. Xiangguang Li

E-mail addresses: xgl@gdut.edu.cn

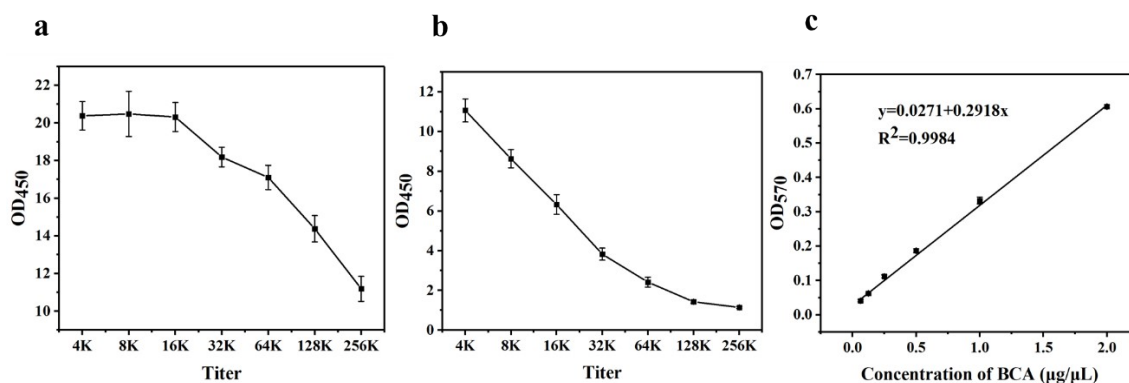
Prof. Suqing Zhao

E-mail addresses: sqzhao@gdut.edu.cn

E-mail addresses for other authors

2111906111@mail2.gdut.edu.cn (Shan Liang), grana233@163.com (Ji
Li), gdutchemzyy@163.com (Yingying Zhong),
ttwang2314163620@163.com (Tiantian Wang), iyihgnay@163.com
(Huiyi Yang)

22 Evaluation of the anti-*L. monocytogenes* pAbs

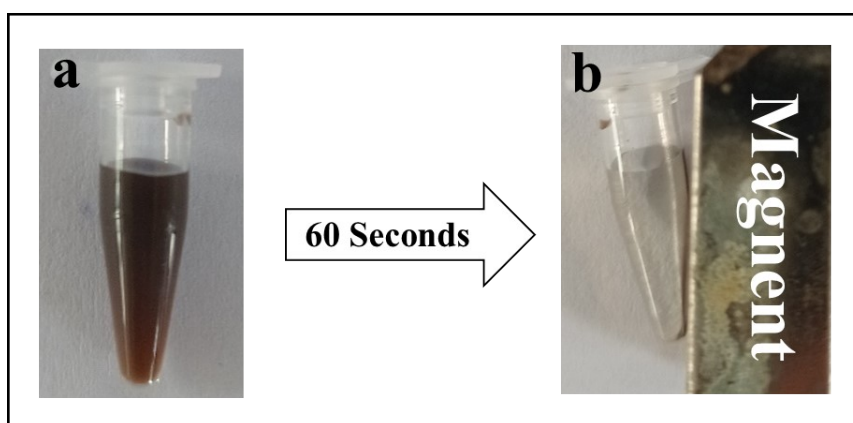


23

24 **Fig. S1.** The titer of the anti-*L. monocytogenes* (a) rabbit antibody and (b)
25 guinea pig antibody after the fourth injection (n=3) by the method of
26 iELISA method. (c) The standard protein curve of BCA. The concentration
27 of anti-*L. monocytogenes* rabbit and guinea pig antibody is 10 µg/µL,
28 respectively.

29

30 Characterization of Fe₃O₄ NPs



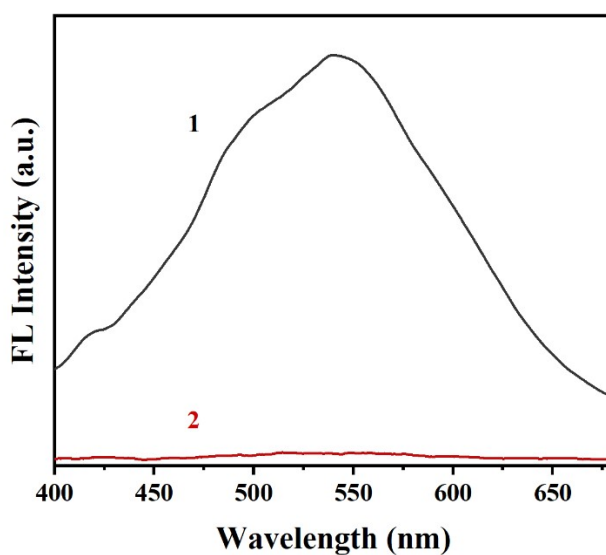
31

32 **Fig. S2.** Photographs of Fe₃O₄ nanoparticles in water taken before (a) and
33 after (b) magnetic separation.

34

35

36 Preparation of CdZnTe QDs and CdZnTe QDs/pAb2



37

38 **Fig. S3.** Fluorescence spectra of CdZnTe QDs in deionized water (Line 1)
39 and the supernatant of CdZnTe QDs after centrifugation (Line 2).

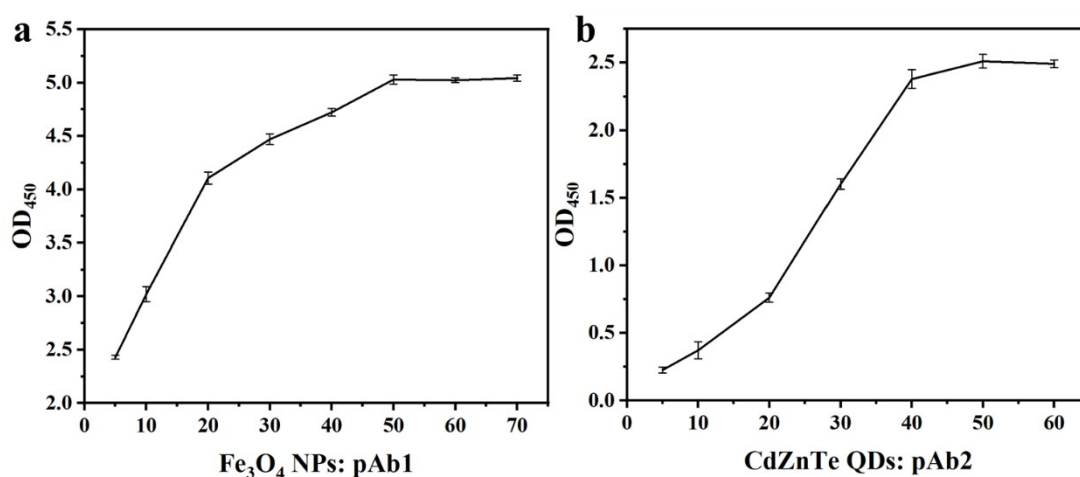
40

41 Optimization of the concentration ratio of Fe₃O₄ NPs to pAb1 and 42 CdZnTe QDs to pAb2

43 To optimize the concentration ratio of Fe₃O₄ NPs to pAb1, Fe₃O₄ NPs (2.9
44 mg mL⁻¹) with different volumes (50, 100, 200, 300, 400, 500, 600 and 700
45 μL) was mixed with 10 μL pAb1 (10.0 mg mL⁻¹) and the mixture was
46 stirred for 24 hours at 4 °C. After washing three times with PBS (10 mM,
47 pH 7.4), Fe₃O₄ NPs/pAb1 was collected with centrifuging at 10000
48 rpm/min for 15 min. Then, the Fe₃O₄ NPs/pAb1 was been added to HRP-
49 goat anti-guinea pig secondary antibodies diluted 1: 5000 with PBS and
50 cultivated at 37 °C for 1 hour. Finally, the mixture was washed three times
51 under the same conditions as before and the optical density (OD) values at

52 a wavelength of 450 nm were measured by a Thermo Scientific microplate
53 reader.

54 With the purpose to obtain the optimal concentration ratio of CdZnTe
55 QDs to pAb2, 120 mg of EDC·HCl and 18 mg of NHS were mixed with
56 CdZnTe QDs (5 mL, 6.9 mg mL⁻¹) with vigorous shaking for 15 minutes
57 at room temperature. After that, 10 μL of pAb2 (10.0 mg mL⁻¹) was added
58 into the above mixture with different volumes (50, 100, 200, 300, 400, 500
59 and 600 μL) which was stirred for another 24 h at 4 °C. Finally, the
60 obtained CdZnTe QDs/pAb2 were washed by centrifugation (10000 rpm,
61 5 minutes) and dispersed in HRP-goat anti-rabbit secondary antibodies
62 diluted 1: 5000 with PBS and cultivated at 37 °C for 1 hour. The optical
63 density (OD) values at a wavelength of 450 nm were measured by a
64 Thermo Scientific microplate reader.



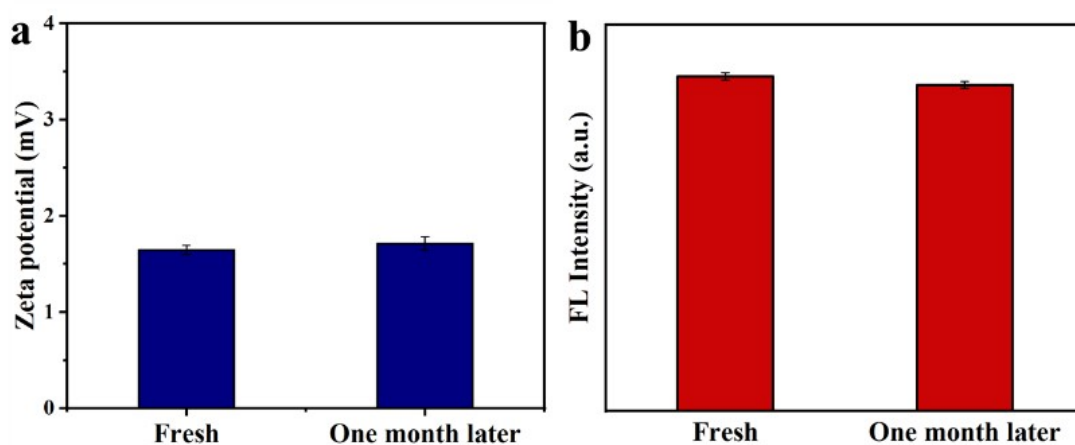
65
66 **Fig. S4.** The optimization of volume ratio of Fe₃O₄ NPs to pAb1 (a) and
67 CdZnTe QDs to pAb2 (b).

68 As shown in Fig. S4, the OD value of the antigen-antibody complex

69 gradually increased with the volume ratio of Fe_3O_4 NPs: pAb1 and CdZnTe
70 QDs: pAb2, and plateaued starting at 50, respectively. The results indicated
71 that the optimal volume ratio of Fe_3O_4 NPs to pAb1 and CdZnTe QDs to
72 pAb2 was 50. When the binding rate peaked, the binding site was filled up
73 and no more coupling took place.

74

75 **The stability of the Fe_3O_4 NPs/ pAb1 and QDs/pAb2**



76

77 **Fig. S5.** The zeta potential (mV) of the Fe_3O_4 NPs/pAb1 sample (a) and
78 FL intensity of the CdZnTe QDs/pAb2 sample (b), freshly prepared and
79 stored for one month, respectively.

80

81

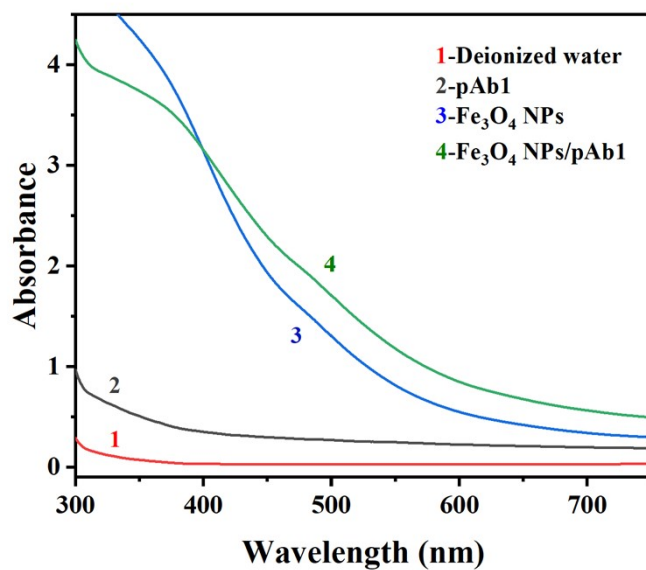
82

83

84

85

86 Characterization of Fe₃O₄ and Fe₃O₄ NPs/pAb1

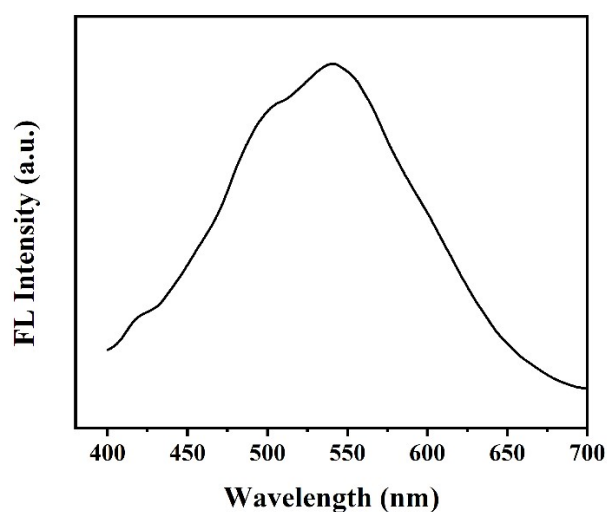


87

88 **Fig. S6.** UV-vis absorption spectra of the deionized water (line 1), the
89 pAb1 (10.0 mg mL⁻¹, line 2) and the Fe₃O₄ NPs (2.725 mg mL⁻¹, line 3)
90 and the Fe₃O₄ NPs/pAb1 (line 4).

91 As shown in Fig. S6, the UV-vis absorption spectra of the free pAb1, Fe₃O₄
92 NPs and Fe₃O₄ NPs/pAb1 exhibited no characteristic UV-vis peak.

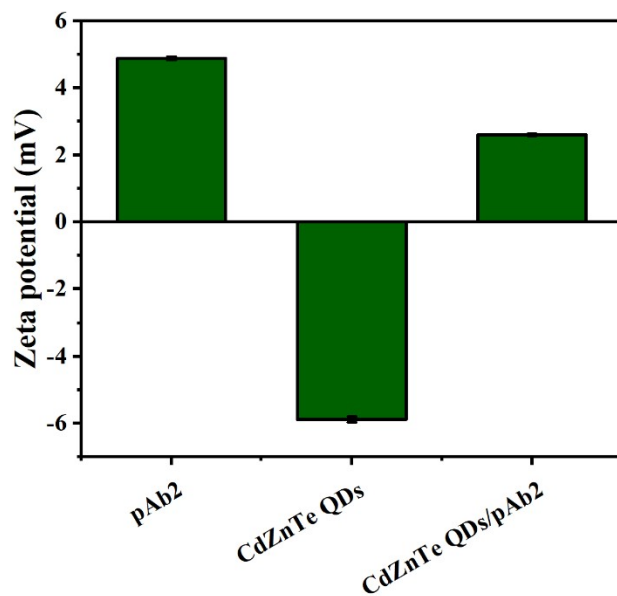
93 Characterization of CdZnTe QDs and CdZnTe QDs/pAb2



94

95 **Fig. S7.** Fluorescence spectrum of CdZnTe QDs/pAb2

96



97

98 **Fig. S8.** Zeta potentials of the pAb2, the CdZnTe QDs and the CdZnTe
99 QDs/ pAb2.